NASA TECHNICAL TRANSLATION NASA TT F-14,230

CURLING OF AN UNSTABLE DISCONTINUITY SURFACE

H. Kaden

Translation of: "Aufwicklung einer unstabilen Unstetigkeitsfläche", Ingenieur-Archiv Gesellschaft fuer Angewandte Mathematik und Mechanik, Vol. 2, 1931, pp. 140-168.

NATIONAL AERONAUTICS AND SPACE ADMINISTRATION
WASHINGTON, D. C. 20546 MARCH 1972

CURLING OF AN UNSTABLE DISCONTINUITY SURFACE[1]

H. Kaden

ABSTRACT. The unstable vortex layer behind a wing is analyzed using conformal mapping techniques. A plane discontinuity model is developed and the rolling-up process of the surface is studied. Applications to airfoil wing theory are given. A corresponding flow visualization experiment in a water tank is described.

Summary of the most important designations: /140*

The meanings are:

Γ	the circulation
Γ_0	the circulation of the spiral core
x, y or ξ, η	rectangular coordinates
r, φ	polar coordinates
u, v	horizontal and vertical components of velocity
w	absolute magnitude of the velocity vector
$u_t(r, \varphi)$	circumferential velocity of the flow in the spiral perpendicular to r
v_n	normal component of the velocity with which the separation surface moves
v_r	radial component of the flow velocity in the spiral
t	time
P	force on the vortex surface
ϱ	density of the fluid
p	fluid pressure
γ	angle between the radius and the positive tangent direction of the spiral
ν	exponent in the equation of the spiral

[1] Dissertation, Göttinger; Prof. Dr. A. Betz, adviser.

*Numbers in the margin indicate pagination in the original foreign text.

$X_0 = x_0 t^{\frac{2}{3}}$	that section of the unperturbed vortex surface for which the circulation is equal to Γ_0
a	horizontal distance of the midpoint of the spiral from the starting point of the unperturbed section of the vortex
b	vertical distance of the midpoint of the spiral from the unperturbed vortex section
U	horizontal component of the velocity of the midpoint of the spiral
V	vertical component of the velocity of the midpoint of the spiral
$\sigma = \frac{\Gamma}{2\sqrt{\nu}}$	measure of the intensity of the vortex surface
$\varkappa = \frac{\Gamma}{2\sqrt{\nu}} = k_1 \pi$, $k = (\varkappa \pi)^{\frac{2}{3}}$	measure for the intensity of the vortex core

I. INTRODUCTION

1. Technical Problem

With airfoils such as are used for the lifting surfaces of aircraft, a vortex layer forms behind the wing, moving out from the trailing edge. In the case of vanishingly small viscosity, this degenerates into a mathematical discontinuity surface. As a result of the pressure distribution at the lateral ends of the wing, that is, the part flowing along the suction surface experiences an acceleration away from the lateral end of the wing, while that flowing along the pressure side is accelerated toward the end. Then if the parts of the fluid meet again at the trailing edge of the wing, one has a velocity component toward the inside, and the other — a component toward the outside. A discontinuity surface has formed at the boundary (Figure 1). Airfoil theory is intensively concerned with the

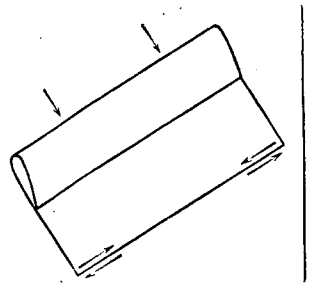

Figure 1. Discontinuity surface behind a wing.

flow field of this vortex layer, so that it has been able to explain the effect of the ends of the wing on the drag of the wing (induced drag) in detail and in very good agreement with / 141
experience. Among other things, it has been possible to show that the induced drag is at a minimum for a given lift if the lift is distributed so that the discontinuity surface behind the wing has the same downward velocity at all points, so that it does not become deformed, but remains flat.

But such a flat vortex surface is not stable. Its lateral edges have the tendency to roll inward (Figure 2; see also the motion picture frames in Figure 23). In the simplest form of airfoil theory, it is assumed that this process of rolling in proceeds very slowly, so that one can consider the vortex surface to be flat for theoretical treatment of flow in the vicinity of the wing. If the lift of the wing is made small enough, this requirement can be fulfilled. Now in practice the conditions are such that, for most problems which relate to processes at the wing itself, the effect of this curling of the discontinuity surface can be neglected, but it is important for processes somewhat behind the wing, as for the aircraft elevators. More accurate knowledge of this process may be even more important for application of airfoil theory in machine design (turbines, centrifugal pumps) than for aerodynamic problems. As already mentioned, in aerodynamic problems the assumption of simple airfoil theory that the perturbing motions are small in comparison to the principal motion is at least to some extent fulfilled, but this is almost never the case for problems in machine technology.

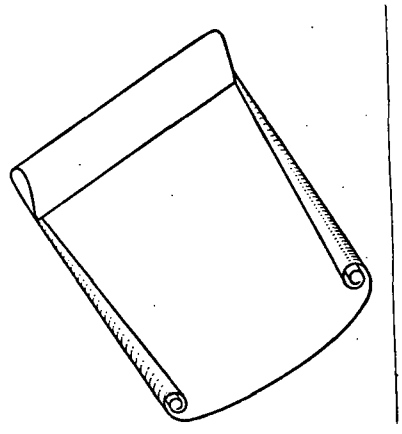

Figure 2. Curling of the discontinuity surface.

Then such processes as the curling of the discontinuity surfaces play a much greater role than in aerodynamic problems. For that reason there has for a long time been a practical interest in understanding the process of curling. The present investigation is aimed at that objective[2].

2. Simplification of the Problem

We shall limit ourselves to following the process in its first stage, in which the extent of the curled surface is still very small in comparison to the wing span, so that we need consider only one side of the wing, while the other may be extended to infinity. Further, we shall assume the process to proceed so slowly in comparison to the flight speed of the wing that we can follow it at a great distance from the wing and also, because of the slow change in flight direction, can consider it as flat. So we arrive at the following simpler problem:

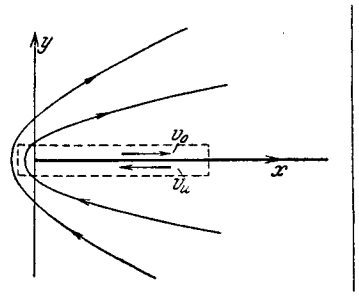

Figure 3. Flow around a discontinuity surface which is plane and extends to infinity at one side.

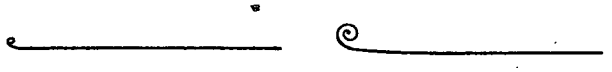

Figures 4 and 5. Curling at the edge of the discontinuity surface.

Given a plane discontinuity surface, extending to infinity at one side, with a distribution of discontinuity occurring with flow about such a surface as shown in Figure 3. Now this surface steadily rolls inward at its free end (Figures 4 and 5).

(2) It was done at the suggestion of Prof. Betz and under his direction.

The time course of this process and the shape of the rolled-up surface are to be investigated. (3)

/ 142

The flow about a rigid surface such as shown in Figure 3 is well known. For instance, one can obtain it easily by the conformal mapping $\zeta = \sigma \sqrt{z}$ from the elementary parallel flow along a plane wall with unit velocity (ζ -plane). At a point at a distance x from the free end of the surface, the velocity above the surface is

$$v_o = \frac{\sigma}{2} \frac{1}{\sqrt{x}} \qquad (1)$$

and below the surface

$$v_u = -\frac{\sigma}{2} \frac{1}{\sqrt{x}}. \qquad (2)$$

The velocity jump or, which is the same thing, the circulation (4) per unit length of the wing is

$$v_o - v_u = \Gamma' = \frac{\sigma}{\sqrt{x}}. \qquad (3)$$

Therefore, the circulation about the whole segment of the surface from the starting point to point x (integral across the dashed line in Figure 3) becomes

$$\Gamma = \oint v_s \, ds = \int_0^x \Gamma' \, dx = \sigma \int_0^x \frac{dx}{\sqrt{x}} = 2\sigma \sqrt{x}. \qquad (4)$$

Here the factor σ is a measure of the intensity of the vortex surface. It is established for processes behind a wing of finite span by the downward velocity of the discontinuity surface or by the magnitude of the lift of the wing. For

(3) Such curling discontinuity surfaces also appear in other cases, as in the downflow behind an edge. Prandtl has already treated the particularly simple case in which the curling surface has the shape of a logarithmic spiral. L. Prandtl, On the Origin of Vortices in an Ideal Fluid (Karman-Levi, Civita, Lectures on the area of Hydrodynamics and Aerodynamics, Berlin, 1924).

(4) By circulation, we mean the value of the closed line integral $\oint v_s \, ds$.

infinite span width, which we assume here, however, this relation loses its meaning, as with arbitrarily increasing span the downward velocity of the discontinuity surface approaches zero.

3. Similarity Laws

By moving one edge of the discontinuity surface to infinity, we have gained an important advantage in treating the problem. That is, since no explicit length appears in the entire flow region, so that the process is independent of any scale, the resulting flow forms are all similar during the curling of the separation surface. The time course is simply a continuous similar enlargement of a certain flow shape. Because of the importance of this understanding for the entire broader treatment of the problem, we shall go into this point in somewhat more detail.

First, it is easily seen that in the end flow (Figure 3) there remains a similarity relation in itself. At a point at a distance x from the edge (the zero point) the velocity is $v_1 = \pm\frac{\sigma}{2}\frac{1}{\sqrt{x}}$. If we go n times as far, then the velocity is $v_2 = \pm\frac{\sigma}{2}\frac{1}{\sqrt{nx}} = \frac{v_1}{\sqrt{n}}$. That means that the ratio $\frac{v_1}{v_2} = \sqrt{n}$ depends only on the ratio of the distances from the zero point, and not on the absolute magnitudes of the distances. As this applies for all points of the discontinuity surface, and this makes up the only boundary in the flow, this law must also be valid in the interior of the flow, because the velocities in / 143
the interior are unambiguously determined by those at the boundary. Thus, we can also derive directly the similarity law for the interior, in which we calculate the velocities by means of the conformal mapping (Figure 6):

$$w = \sqrt{u^2 + v^2} = \frac{1}{2}\frac{\sigma}{\sqrt{r}}, \qquad \frac{v}{u} = \operatorname{tg}\frac{\varphi}{2}. \tag{5}$$

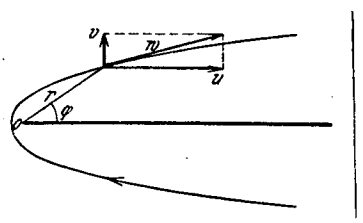

Figure 6. Velocities in flow around the plane discontinuity surface.

From this we see that in points placed analogously to the zero point (φ = constant) the velocities decrease in proportion to $1/\sqrt{r}$ and their directions are constant. That is, the similarity relation is fulfilled in the entire space.

Now let us consider two similar regions separated out of this initial flow, one of which has dimensions n times as large as the other, and consider the changes appearing in each. As all the initial velocities are also proportional to each other at analogously placed points, so too, every mutual displacement of points in the two regions is similar to each other. Therefore, exactly similar changes of shape appear in the flow lines in the two regions. The corresponding process in the large region only lasts longer than in the small one, as, on one hand, the velocities are smaller by the factor $1/\sqrt{n}$ and the distances covered are n times as large as in the smaller region. The time necessary to attain a similar change in shape in the large region is, therefore, $n\sqrt{n} = n^{\frac{3}{2}}$ times longer than in the small region. Thus, we obtain the result that a flow picture which appears at a time t calculated from the beginning of the movement is again present at the time $n^{3/2}t$ in n-fold increased scale. From this it appears that the times t_1 and t_2 have the following relations to the scales r_1 and r_2 of the similar flow pictures:

$$\frac{t_2}{t_1} = n^{\frac{3}{2}} = \left(\frac{r_2}{r_1}\right)^{\frac{3}{2}} \quad \text{or} \quad \frac{r_2}{r_1} = \left(\frac{t_2}{t_1}\right)^{\frac{2}{3}}. \tag{6}$$

Accordingly, we can also formulate our problem in this way: We are to find the shape and the behavior of a spiral which enlarges according to the time law above. In this we can proceed essentially by considering the spiral as being produced by a fixed, mechanically extended wall. The flow can be determined for an arbitrarily prescribed shape of the wall. The correct shape of the spiral then arises from the condition that there may not be pressure differences at the two sides of the spiral, as it is really not fixed, but only represents a discontinuity surface which cannot maintain any pressure difference.

In the following calculations we shall not start from the flow shown in Figure 3, but from the opposite flow — that is, from a flow which moves around the discontinuity surface in a counterclockwise direction. This basis proves to be more expedient for the mathematical representation, because we are now in agreement with the usual representation of spirals. Now our separation surface coils up underneath.

II. BEHAVIOR IN THE INTERIOR OF THE SPIRAL

1. General Considerations

If we draw a circle of radius r about the midpoint of the spiral, the line integral of the velocity along this circle is identical to the circulation L about the portion of the discontinuity surface lying within the circle. Accordingly, the mean circumferential velocity $\bar{u}_t$ is

$$\bar{u}_t = \frac{\Gamma}{2\pi r}; \tag{7}$$

and the mean angular velocity of a particle at distance r is / 144

$$\bar{\omega} = \frac{\bar{u}_t}{r} = \frac{\Gamma}{2\pi r^2}.$$

If the circulation in the spiral were distributed so that the mean circulation per unit area were constant, then $\bar{\omega} = \frac{\Gamma}{2\pi r^2}$ would be independent of r. Then the fluid would circulate with constant angular velocity, i. e., like a rigid body. But because the inner parts of the spiral are derived from those parts of the original discontinuity surface which were near the edge itself, where the circulation per unit length, Γ', was particularly large [$\Gamma' = \frac{\sigma}{\sqrt{\varkappa}}$; see Equation (3)] it must from the beginning be assumed that in the spiral also the spatial density of the circulation $\frac{\Gamma}{2\pi r^2}$ and, thus, of the angular velocity, is greater in the inside than at the outside. But if one curls up a surface so that the angular

velocity is greater in the inside than at the outside, the number of coils increases steadily. The individual coils are more and more closely packed, and more and more approximate concentric circles. So we must expect that our discontinuity surface, curling up toward the center, has increasingly narrower and more circular coils. This qualitative behavior is also confirmed by observation.

Since no new discontinuities appear in the interior, the circulation about a circle around the midpoint can change with time only if parts of the discontinuity surface move into or out of the circle. Such transport of vortices of the discontinuity surface can only occur in the degree to which radial velocity components are present. As just as much fluid must leave the circle as enters it, on the grounds of continuity, the mean radial velocity component is zero. Vortex transport can, therefore, arise only from local deviations from the mean velocity. But these deviations become smaller, the closer together the turns of the spiral are and the more circularly symmetrical they become. This is, as we saw previously, more exactly the case the nearer we approach the midpoint. Thus, the radial velocity components vanish in the vicinity of the midpoint, and the circulation for a certain circle remains constant with time. Of course, the peripheral velocity also remains unchanged with time. Then these quantities depend only on the radius.

2. Calculation For a First Approximation

This knowledge, along with the similarity relation mentioned in the introduction, provides evidence on the form of the spiral in the vicinity of the midpoint. Due to the close coils in the neighborhood of the midpoint, the velocity is constant along a circle around the midpoint. Thus, we need not differentiate between the mean velocity $\bar{u}_t$ on the circumference of the circle and the velocity u_t at any point of the circle. According to the similarity law [Equation (6)]

the relation of the velocity u_{t_1} at radius r_1 and time t_1 to the velocity u_{t_2} at radius r_2 and time $t_2 = t_1)r_2/r_1)^{3/2}$ is

$$\frac{u_{t_1}}{u_{t_2}} = \left(\frac{r_2}{r_1}\right)^{\frac{1}{2}}. \quad (8)$$

But since the velocities in the vicinity of the midpoint are independent of time, this ratio applies not only for the times t_1 and t_2 but for all times. In this way we obtain the general relations

$$u_t = \frac{k_1}{\sqrt{r}}$$

and

/ 145

$$\Gamma = u_t 2\pi r = 2k_1\pi\sqrt{r} = 2\varkappa\sqrt{r}. \quad (9)$$

The distribution of Γ along the radius in the coiled state is therefore entirely analogous to the original distribution ($\Gamma = 2\sigma\sqrt{x}$). The relation between $\varkappa$ and σ is yet to be determined in Chapter IV.

Now we consider one coil of the spiral. In its analogous enlargement, the space enclosed by it and the radial connecting segment Δr between the coil ends expands (Figure 7). Because no fluid passes through the spiral surface, which is made up always of the same fluid particles, the entire amount of fluid, Q, needed to enlarge the space must flow in through the radial connecting segment Δr . Accordingly, we have the relation

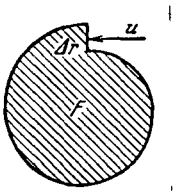

Figure 7. Region enclosed by one turn of the spiral.

$$Q = u_t \Delta r = \frac{dF}{dt}.$$

For nearly circular coils, such as we have near the midpoint, $F = \pi r^2$. According to the expansion law given in the

introduction [Equation (6)],

$$r = r_1 t^{\frac{2}{3}} \quad \text{or} \quad \frac{dr}{dt} = \frac{2}{3} r_1 t^{-\frac{1}{3}} = \frac{2}{3} \frac{r}{t},$$

consequently

$$\frac{dF}{dt} = 2\pi r \frac{dr}{dt} = \frac{4\pi}{3} \frac{r^2}{t}.$$

Therefore,

$$\Delta r = \frac{\frac{dF}{dt}}{u_i} = \frac{4\pi r^2}{3t} \frac{\pi \sqrt{r}}{\varkappa} = \frac{4}{3} \frac{\pi^2}{\varkappa} \frac{r^{\frac{5}{2}}}{t}.$$

As long as $\Delta r/r$ varies only slightly from coil to coil, as is naturally the case with very close windings, we have

$$\Delta r = -2\pi \frac{\partial r}{\partial \varphi},$$

in which r and φ are the polar coordinates of the spiral. Now if we insert the value above for Δr, we obtain

$$\frac{\partial r}{\partial \varphi} = -\frac{2}{3} \frac{\pi}{\varkappa} \frac{r^{\frac{5}{2}}}{t}$$

or, integrated,

$$t \frac{\varkappa}{\pi} r^{-\frac{3}{2}} = \varphi,$$

or

$$r = \left(\frac{\varkappa t}{\pi \varphi}\right)^{\frac{2}{3}}. \qquad (11)$$

3. Calculation for the Second Approximation

If we draw such a spiral (shown dashed in Figure 19), then by comparison with Figures 4 and 5 (or 19 and 23) we see at once that extrapolation of this form derived for the neighborhood of the midpoint to large radii r (small φ) does not agree with the desired spiral. Therefore, the formula above (11) is only

an approximation for the vicinity of the midpoint. Now we must ask how far this approximation applies and how another approximation for larger radii can be sought. For this purpose we generalize Equation (11) by substituting a general φ for the exponent of r instead of the value 2/3 which is valid for the midpoint, and attempt to determine the change of this exponent approximately. Thus, we set up the following formula for the spiral

$$r = \left(\frac{\varkappa t}{\pi}\right)^{\frac{2}{3}} \frac{1}{\varphi^{\nu}} = k \frac{t^{\frac{2}{3}}}{\varphi^{\nu}}, \qquad (12)$$

in which, for brevity, we set $\left(\frac{\varkappa}{\pi}\right)^{\frac{2}{3}} = k$, and ν should be a function of φ so that $\nu \to \frac{2}{3}$ as $\varphi \to \infty$. With this formula, we will now follow the flow linked to the analogous enlargement. But now we must be free of the simplifying assumptions which apply only for very close windings. We must assume:

1. that the radius changes markedly in the course of one turn, and that the velocity u_t is variable not only along a circle about the midpoint but also along a radius between two adjacent turns (along Δr). Thus, in place of the expressions $F = \pi r^2$, $\Gamma = u_t 2\pi r$ and $Q = u_t \Delta r$ the appropriate integrals now appear.

2. that the circulation within a circle of given radius is no longer constant with time, because of the occurrence of radial velocities.

But we shall limit ourselves to a region in which these deviations from the previous assumptions are not yet very large, so that we can still allow many simplifications in the calculation. In particular, we shall assume:

1. that the exponent ν changes so slowly that we can take it to be constant to some degree, at least in a range from φ to $\varphi + 2\pi$.

2. that the radial velocity components are very small in comparison to the tangential ones, i.e., that the paths of the fluid particles depart only very slightly from circles.

We proceed from Equation (10), according to which

$$\Delta r\, u_t = \frac{dF}{dt}$$

For dF/dt, however, we calculate the exact value

$$\frac{dF}{dt} = \int_{\varphi-2\pi}^{\varphi} v_n\, ds, \qquad (13)$$

in which v_n is the normal component of the velocity with which one point of the spiral moves in the analogous enlargement, and ds is the arc element along the spiral (Figure 8). We also consider now the change of the peripheral velocity u_t over the cross section Δr. That is, instead of Equation (10) we write the relation

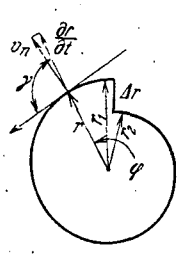

Figure 8

$$\int_{r_2}^{r_1} u_t\, dr = \int_{\varphi-2\pi}^{\varphi} v_n\, ds. \qquad (14)$$

If no radial velocities were present, and if each liquid particle moved on circular paths about the common midpoint, then, as potential flow prevails here and the radial velocities are assumed to be very small, the relation for the dependence on radius between two spiral surfaces would be

$$u_t = c\frac{1}{r}, \qquad (15)$$

in which $c(\varphi)$ must be determined from Equation (14).

If we define γ as the angle between the radius vector and the positive direction of tangent T to the spiral (Figure 9), then / 147

$$v_n = \frac{\partial r}{\partial t}\sin\gamma = \frac{2}{3}\,k\,t^{-\frac{1}{3}}\frac{\sin\gamma}{\varphi^{\gamma}}$$

and

$$ds = \frac{r\,d\varphi}{\sin\gamma} = k\,\frac{t^{\frac{2}{3}}\,d\varphi}{\varphi^{\gamma}\sin\gamma}.$$

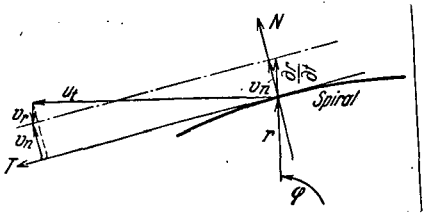

Figure 9. Analysis of the velocities.

Now, accordingly, we obtain

$$\int_{\varphi-2\pi}^{\varphi} v_n\, ds = \frac{2}{3} k^2 t^{\frac{1}{3}} \int_{\varphi-2\pi}^{\varphi} \frac{d\varphi}{\varphi^{2\nu}} = \frac{2}{3} k^2 \frac{t^{\frac{1}{3}}}{2\nu-1}\left[\frac{1}{(\varphi-2\pi)^{2\nu-1}} - \frac{1}{\varphi^{2\nu-1}}\right]$$

$$= \frac{2}{3} k^2 t^{\frac{1}{3}}\left[\frac{2\pi}{\varphi^{2\nu}} + \nu\frac{(2\pi)^2}{\varphi^{2\nu+1}} + \frac{(2\nu+1)\nu}{3}\frac{(2\pi)^3}{\varphi^{2\nu+2}} + \cdots\right]; \qquad (16)$$

Here ν is considered to be sufficiently constant in the integration interval, in agreement with the assumptions stated.

Furthermore, Equation (15) yields

$$\int_{r_2}^{r_1} u_t\, dr = c\int_{r(\varphi)}^{r(\varphi-2\pi)} \frac{dr}{r} = -c\nu \ln\frac{\varphi-2\pi}{\varphi} = c\nu\left[\frac{2\pi}{\varphi} + \frac{1}{2}\left(\frac{2\pi}{\varphi}\right)^2 + \frac{1}{3}\left(\frac{2\pi}{\varphi}\right)^3 + \cdots\right].$$

So, from Equation (14) we obtain

$$c(\varphi) = \frac{2}{3}\frac{t^{\frac{1}{3}}}{\nu}\frac{k^2}{\varphi^{2\nu-1}}\left[1 + \frac{2\nu-1}{2}\frac{2\pi}{\varphi} + \frac{1}{3}\left(2\nu^2 - \frac{\nu}{2} - \frac{1}{4}\right)\left(\frac{2\pi}{\varphi}\right)^2 + \cdots\right]$$

and with it

$$u_t(r,\varphi) = \frac{c(\varphi)}{r} = \frac{2}{3}\frac{t^{\frac{1}{3}}}{\nu}\frac{k^2}{\varphi^{2\nu-1}r}\left[1 + \frac{2\nu-1}{2}\frac{2\pi}{\varphi} + \frac{1}{3}\left(2\nu^2 - \frac{\nu}{2} - \frac{1}{4}\right)\left(\frac{2\pi}{\varphi}\right)^2 + \cdots\right]. \qquad (17)$$

In order to obtain the radial component of the flow velocity, v_r, we must introduce the condition that the normal component of the velocity with which the separation surface moves must be equal to the component of the flow velocity in the normal direction. Thus, from Figure 9 there appear the relations

$$-u_t\left(r = \frac{k\,t^{\frac{2}{3}}}{\varphi^{\nu}}, \varphi\right)\cos\gamma + v_r\left(r = \frac{k\,t^{\frac{2}{3}}}{\varphi^{\nu}}, \varphi\right)\sin\gamma = v_n = \frac{\partial r}{\partial t}\sin\gamma$$

and

$$-u_t\left(r = \frac{k\,t^{\frac{2}{3}}}{\varphi^{\nu}}, \varphi + 2\pi\right)\cos\gamma + v_r\left(r = \frac{k\,t^{\frac{2}{3}}}{\varphi^{\nu}}, \varphi + 2\pi\right)\sin\gamma = \frac{\partial r}{\partial t}\sin\gamma;$$

for the two sides of the discontinuity surface.

With Equation (17) and

$$\operatorname{tg}\gamma = r\frac{\partial\varphi}{\partial r} = -\frac{\varphi}{\nu}$$

these become

$$v_r\left(r = \frac{kt^{\frac{2}{3}}}{\varphi^{\nu}},\ \varphi\right) = -\frac{2}{3}kt^{-\frac{1}{3}}\left[\frac{2\nu-1}{2}\frac{2\pi}{\varphi^{\nu+1}} + \frac{1}{3}\left(2\nu^2 - \frac{\nu}{2} - \frac{1}{4}\right)\frac{(2\pi)^2}{\varphi^{\nu+2}} + \cdots\right] \tag{18}$$

and

$$v_r\left(r = \frac{kt^{\frac{2}{3}}}{\varphi^{\nu}},\ \varphi + 2\pi\right) = +\frac{2}{3}kt^{-\frac{1}{3}}\left[\frac{2\nu-1}{2}\frac{2\pi}{\varphi^{\nu+1}} - \frac{1}{3}\left(2\nu^2 - \frac{\nu}{2} - \frac{1}{4}\right)\frac{(2\pi)^2}{\varphi^{\nu+2}} + \cdots\right]. \tag{19}$$

Now we are in a position to calculate the circulation Γ which occurs within a circle of radius r. This is equal to the value of the line integral of the velocity along an arbitrary closed curve: / 148

$$\Gamma = \oint v_s\, ds.$$

As the peripheral velocities $u(r,\varphi)$ are known from Equation (17) in our case, it is convenient to choose the circle of radius r as the closed curve in the above integral for Γ, and we obtain

$$\begin{aligned}\Gamma &= \int_{\varphi}^{\varphi+2\pi} u_t(r,\varphi)\, r\, d\varphi = \int_{\varphi}^{\varphi+2\pi} c(\varphi)\, d\varphi \\ &= \frac{2}{3}t^{\frac{1}{3}}\frac{k^2}{\nu}\int_{\varphi}^{\varphi+2\pi}\frac{d\varphi}{\varphi^{2\nu-1}}\left[1 + \frac{2\nu-1}{2}\frac{2\pi}{\varphi} + \frac{1}{3}\left(2\nu^2 - \frac{\nu}{2} - \frac{1}{4}\right)\left(\frac{2\pi}{\varphi}\right)^2 + \cdots\right] \\ &= \frac{2}{3}\frac{t^{\frac{1}{3}}}{\nu}\frac{k^2}{\varphi^{2\nu-2}}\left[\frac{2\pi}{\varphi} + \left(\frac{1}{3}\nu^2 - \frac{1}{12}\right)\left(\frac{2\pi}{\varphi}\right)^2 + \cdots\right].\end{aligned} \tag{20}$$

Since $r = \frac{kt^{\frac{2}{3}}}{\varphi^{\nu}}$, we obtain from (20) the circulation as a function of the radius r and the time t:

$$\Gamma(r,t) = \frac{2}{3}\frac{1}{\nu}\left(2\pi k^{\frac{1}{\nu}}\frac{r^{2-\frac{1}{\nu}}}{t^{1-\frac{2}{3}\frac{1}{\nu}}} + \frac{(2\pi)^3}{k^{\frac{1}{\nu}}}\frac{r^{2+\frac{1}{\nu}}}{t^{1+\frac{2}{3}\frac{1}{\nu}}}\left(\frac{1}{3}\nu^2 - \frac{1}{12}\right) + \cdots\right]. \tag{21}$$

Now a change of Γ in the circle of constant radius r can take place only to the extent that vortices move into or out of this circle. This vortex transport out of the circle is, according to Helmholtz, equal to the mean radial flow velocity $\frac{1}{2}[v_r(r,\varphi)+v_r(r,\varphi+2\pi)]$ multiplied by the increase of circulation in the radial direction. Thus, the relation must be

$$\frac{\partial\Gamma}{\partial t}=-\frac{\partial\Gamma}{\partial r}\cdot\frac{1}{2}[v_r(r,\varphi)+v_r(r,\varphi+2\pi)], \qquad (22)$$

in which the minus sign must be placed on the right side because the circulation decreases with positive, i. e., outwardly directed, radial velocity v_r. Then if we differentiate Equation (21) with respect to t and r, taking the value for v_r from Equations (18) and (19), we obtain from Equation (22)

$$\frac{2}{3}\frac{1}{\nu}\left[2\pi k^{\frac{1}{\nu}}\frac{\nu^{2-\frac{1}{\nu}}}{t^{2-\frac{2}{3}\frac{1}{\nu}}}\left(\frac{2}{3}\frac{1}{\nu}-1\right)-\frac{(2\pi)^3}{k^{\frac{1}{\nu}}}\frac{r^{2+\frac{1}{\nu}}}{t^{2+\frac{2}{3}\frac{1}{\nu}}}\left(1+\frac{2}{3}\frac{1}{\nu}\right)\left(\frac{1}{3}\nu^2-\frac{1}{12}\right)+\cdots\right]$$

$$=\frac{2}{3}\frac{1}{\nu}\left[2\pi k^{\frac{1}{\nu}}\frac{r^{1-\frac{1}{\nu}}}{t^{1-\frac{2}{3}\frac{1}{\nu}}}\left(2-\frac{1}{\nu}\right)+\frac{(2\pi)^3}{k^{\frac{1}{\nu}}}\frac{r^{1+\frac{1}{\nu}}}{t^{2+\frac{2}{3}\frac{1}{\nu}}}\left(\frac{1}{3}\nu^2-\frac{1}{12}\right)\left(2+\frac{1}{\nu}\right)+\cdots\right]$$

$$\frac{2}{9}\frac{(2\pi)^2}{k^{\frac{2}{\nu}}}\left(2\nu^2-\frac{\nu}{2}-\frac{1}{4}\right)\frac{r^{1+\frac{2}{\nu}}}{t^{\frac{2}{3}+\frac{4}{3}\frac{1}{\nu}}}.$$

Now if we again express r by φ by means of the relation $r=k\frac{t^{\frac{2}{3}}}{\varphi^{\nu}}$, after a brief transformation we obtain, as a first approximation

$$\frac{2}{3}-\nu=\left[\frac{2}{9}(2\nu-1)\left(2\nu^2-\frac{\nu}{2}-\frac{1}{4}\right)+\left(\nu+\frac{2}{3}\right)\left(\frac{1}{3}\nu^2-\frac{1}{12}\right)\right]\left(\frac{2\pi}{\varphi}\right)^2$$

or / 149

$$\left(\frac{2\pi}{\varphi}\right)^2=\frac{\frac{2}{\nu}-3}{\frac{11}{3}\nu^2-\frac{4}{3}\nu-\frac{1}{4}}. \qquad (23)$$

The dependence of the exponent ν on angle φ which arises from this is plotted in Figure 10. We can see that the exponent becomes smaller than 2/3 for the final value of ν. But the change of φ with decreasing angle is rather small, so that in this respect our assumption is fulfilled fairly extensively. For example, $\nu \approx 0{,}65$ when $\varphi = 4\pi$, and for $\varphi = 2\pi$ we still have $\nu \approx 0{,}61$. For this point, to be sure, our approximate calculation is no longer sufficient.

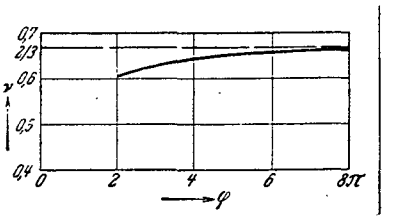

Figure 10. Curve for the exponent ν in equation (12).

For $\varphi < 2\pi$ the exponent ν will decrease even further. For $\varphi = 1$, ν must become $-\infty$. This arises from the following consideration. If r' designates the magnitude of the radius vector which has the exponent $\nu = 2/3$ throughout, so that $r' = \left(\frac{\varkappa t}{\pi\varphi}\right)^{\frac{2}{3}}$, then the ratio becomes

$$\frac{r}{r'} = \varphi^{\frac{2}{3}-\nu} \quad \text{or} \quad \frac{\ln \frac{r}{r'}}{\ln \varphi} = \frac{2}{3} - \nu(\varphi).$$

Now, because this ratio r/r' becomes greater than one for $\varphi = 1$, and ln (r/r') becomes greater than zero, as can be seen from Figure 19, from the formula above ν must become equal to $-\infty$ for ln $\varphi \to 0$. [In the interior of the spiral $(\varphi > 4\pi)$ we can, as a very great approximation, calculate with the exponent $\nu = 2/3$ throughout.]

III. BEHAVIOR OF THE SPIRAL AT INFINITY

1. Vortex Fields in General

The curling of the discontinuity surface takes place from the edge. At a great distance from the edge, the surface at first remains nearly at rest. Thus, the spiral transforms asymptotically into the original straight line. The center of

the spiral, however, moves in relation to this line. For a coordinate system in which the center of the spiral is at the zero point, the equation of this asymptote, and thus the equation of the spiral at a great distance from the midpoint ($\varphi \ll 1$), is

$$r = \frac{b}{\sin \varphi} \approx \frac{b}{\varphi}; \tag{24}$$

where b is the perpendicular distance of the spiral center from the original plane discontinuity surface. It grows with $t^{2/3}$ in the analogous enlargement. We can also give still another approximation to the shape of the spiral for small φ (large r), in which we calculate the departure of the spiral from its asymptote. Here we include the well-known formulas for vortex fields, which we shall summarize briefly here and which we shall use for our problem.

The flow field of a vortex filament from the circulation Γ into a plane, infinitely extended fluid has, for a point at the distance r, the velocity

$$w = \frac{\Gamma}{2\pi r}, \tag{25}$$

the direction of which is perpendicular to the connecting line r from the vortex filament to the point. If the position of the vortex is given by the coordinates ξ, η, and that of the point by x,y, then the components u and v parallel to the x and y axes, respectively, (see Figure 11) are

/ 150

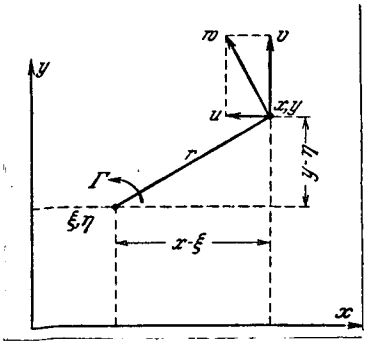

Figure 11. Velocity of a vortex.

$$\left.\begin{aligned} u(x,y) &= -\frac{\Gamma}{2\pi} \frac{y-\eta}{(x-\xi)^2 + (y-\eta)^2}, \\ v(x,y) &= \frac{\Gamma}{2\pi} \frac{x-\xi}{(x-\xi)^2 + (y-\eta)^2}, \end{aligned}\right\} \tag{26}$$

where the circulation Γ is to be considered positive for rotation in the counterclockwise direction. If, instead of a single vortex

filament, there are several with the coordinates ξ_ν, η_ν, their resulting velocity field is given by the formulas

$$\left.\begin{aligned} u(x, y) &= -\frac{1}{2\pi}\sum \frac{\Gamma_\nu (y-\eta_\nu)}{(x-\xi_\nu)^2+(y-\eta_\nu)^2}, \\ v(x, y) &= \frac{1}{2\pi}\sum \frac{\Gamma_\nu (x-\xi_\nu)}{(x-\xi_\nu)^2+(y-\eta_\nu)^2}. \end{aligned}\right\} \tag{27}$$

We shall deal primarily with continuous vortex arrangements, distributed along a curve s with the circulation density $\frac{d\Gamma(s)}{ds}=\Gamma'(s)$ [see, for instance, Equation (1)]. Then these formulas arise for the representation of the velocity field:

$$\left.\begin{aligned} u(x, y) &= -\frac{1}{2\pi}\int_S \frac{\Gamma'(s)(y-\eta(s))\,ds}{(x-\xi(s))^2+(y-\eta(s))^2}, \\ v(x, y) &= \frac{1}{2\pi}\int_S \frac{\Gamma'(s)(x-\xi(s))^2\,ds}{(x-\xi(s))^2+(y-\eta(s))^2}. \end{aligned}\right\} \tag{28}$$

Next we shall apply these to the original linear vortex configuration $\Gamma=2\sigma\sqrt{\xi}$, showing that this at first experiences no change in shape except for its edges, where the curling begins. The effect of a vortex element $d\xi$ at a distance ξ from the edge, with the circulation $d\Gamma=\frac{\sigma}{\sqrt{\xi}}d\xi$ on a point of this band at a distance x (Figure 12) is, according to Equation (26)

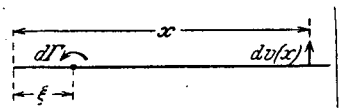

Figure 12. Effect of the continuously distributed vortex on the velocity at a point.

$$du=0, \qquad dv(x)=\frac{d\Gamma(\xi)}{2\pi(x-\xi)},$$

where u and v are the velocity components parallel and perpendicular to the surface. By integration of all the elements, we obtain the total effect of all the vortex elements:

$$v(x)=\frac{1}{2\pi}\int_0^\infty \frac{d\Gamma(\xi)}{x-\xi}=\frac{\sigma}{2\pi}\int_0^\infty \frac{d\xi}{\sqrt{\xi}(x-\xi)}.$$

This is an improper integral, because the integrand becomes infinite for $\xi = x|$. From airfoil theory, where such integrals over discontinuity surfaces often appear, it is known that the physical sense of this integral is given by its so-called principal value. This is

$$v(x) = \frac{2\sigma}{2\pi} \ln 1 = 0. \quad |$$

With this vortex arrangement, then, the effects of all the vortex elements cancel out along the entire discontinuity surface (except for its edge).

2. Effect of the Coiling on the Velocities at a Great Distance

If the vortex surface is coiled up at its edge, then the distribution of the vortex elements in this region is changed, and there appear, as the field of this vortex distribution, / 151
finite perturbation velocities u and v, which result in the further coiling. The curling of the vortex band corresponds to concentration of the vortex in the vicinity of the center of the coil. Therefore, we can express the effect of this process analytically by displacing the vortex from the original flat surface in the direction of this center. If we assume that a vortex element $d\Gamma(\xi)|$ at the distance $\xi|$ is displaced toward the center by the amount $\delta(\xi)|$ - , then the effect of this displacement is the same as that of a vortex couple in Figure 13.

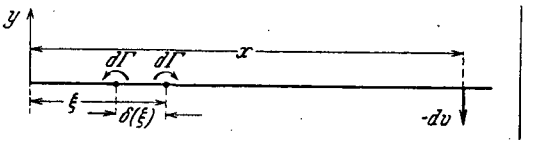

Figure 13. Effect of a horizontal displacement of a vortex.

By addition of such a vortex couple to the original system, the original vortex is canceled by one vortex of the couple, leaving only the second vortex of the couple, and so giving a new system. For the point x which is very far from the displaced vortex, so that $x - \xi \gg \delta(\xi)|$, accordingly, the effect of such a displacement is

$$dv(x) = \frac{1}{2\pi}\left\{\frac{d\Gamma(\xi)}{x-\xi-\delta(\xi)} - \frac{d\Gamma(\xi)}{x-\xi}\right\} \approx \frac{1}{2\pi}\frac{\delta(\xi)\,d\Gamma(\xi)}{(x-\xi)^2}.$$

As the center of force of the vortex remains unchanged in the x-direction (See chapter IV), then for every displacement $\delta(\xi_1)$ of a vortex $d\Gamma(\xi_1)$ to the right, there must occur a corresponding displacement $\delta(\xi_2)$ of a vortex $d\Gamma(\xi_2)$ to the left, so that

$$\delta(\xi_1)\,d\Gamma(\xi_1) = -\delta(\xi_2)\,d\Gamma(\xi_2)$$

The effect of the two displacements is

$$dv(x) = \frac{1}{2\pi}\left\{\frac{\delta(\xi_1)\,d\Gamma(\xi_1)}{(x-\xi_1)^2} + \frac{\delta(\xi_2)\,d\Gamma(\xi_2)}{(x-\xi_2)^2}\right\} \approx -\frac{\delta(\xi_1)\,d\Gamma(\xi_1)}{2\pi}\frac{2(\xi_2-\xi_1)}{x^3}. \qquad (29)$$

Here it is again assumed that $x \gg \xi_1$ as well as $x \gg \xi_2$.

Along with this shift of vortices in the x-direction, there is also a shift in the y-direction. The effect of this can be expressed by a vortex couple according to Figure 14. The field is

$$\left.\begin{aligned} dv(x) &= -\frac{1}{2\pi}\frac{d\Gamma}{x-\xi} + \frac{1}{2\pi}\frac{d\Gamma(x-\xi)}{(x-\xi)^2+\varepsilon^2(\xi)} = -\frac{d\Gamma}{2\pi}\frac{\varepsilon^2(\xi)}{(x-\xi)^3} \approx -\frac{d\Gamma}{2\pi}\frac{\varepsilon^2(\xi)}{x^3}, \\ du(x) &= -\frac{d\Gamma}{2\pi}\frac{\varepsilon(\xi)}{(x-\xi)^2+\varepsilon^2(\xi)} \approx -\frac{d\Gamma}{2\pi}\frac{\varepsilon(\xi)}{x^2}, \end{aligned}\right\} \qquad (30)$$

if $\varepsilon(\xi)$ is the shift of the vortex element $d\Gamma$ in the direction of the negative y-axis. The effect of this shift perpendicular to the x-axis with respect to v(x) decreases, accordingly, with $1/x^3$, and is, therefore, of the same order of magnitude as that according to Equation (29). We obtain the effect of all the vortex shifts by integration over the $d\Gamma(\xi)$, in which the dependence on x is not altered. Thus, for a certain

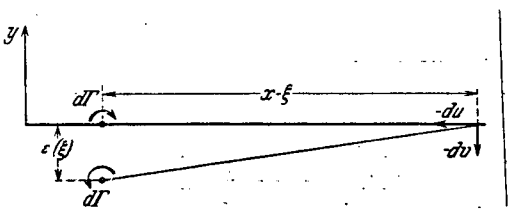

Figure 14. Effect of a perpendicular vortex shift.

point in time we obtain the relation

$$v(x) = \frac{\text{const}}{x^3}. \tag{31}$$

If the exact integration could be performed, it would yield only the value for the constants, which we must temporarily leave undetermined. From Formula (30) we see that the shift of the vortex elements in the y-direction also results in a shift of the vortex in the negative x-direction. We note that this effect diminishes with $1/x^2$, so that our previous assumption that the displacements toward the center of the coil diminish very rapidly with the distance x from the edge is justified. / 152

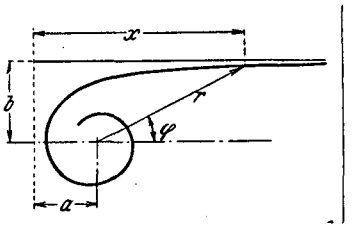

Figure 15

Thus, we know the deviation of our spiral from the straight line, and are in a position to state the analytical form of the separation surface at infinity. From Figure 15 we obtain the following relation

$$b = (x - a)\operatorname{tg}\varphi + \int_0^t v(x)\,dt, \tag{32}$$

where a is the vertical and b the horizontal component of the path which the center of the spiral has traveled up to time t. For sufficiently large x, we can neglect a in comparison to x. Then, on substitution of (31) into (32), the equation for the separation surface becomes

$$\operatorname{tg}\varphi = \frac{b}{x} - \frac{\text{const}}{x^4}; \tag{33}$$

Here b and 'constant' are still functions of the time. From this we see that our spiral clings more closely to the asymptotic straight line than the ordinary hyperbolic spiral $r = \frac{\text{const}}{\varphi}$, because, with the designations above, the

equation for it would be

$$\operatorname{tg}\varphi = \frac{\text{const}}{x} - \frac{\text{const}}{x^3} \cdot \int$$

In this case, the deviation from a straight line enters with the second power of $1/x$, while for our spiral, according to Equation (31), it is proportional to the third power of $1/x$.

IV. DETERMINATION OF THE IMPORTANT CONSTANTS AND ESTABLISHMENT OF THE FORM OF THE SPIRAL

1. Center of Force Rules

A discussion provided by A. Betz proves useful for further treatment. It offers a statement on certain general conditions on the deformation of a vortex surface.

Let us consider the flow realized according to Figure 3 in such a way that we have a rigid material surface (rather like a long thin board) in place of the discontinuity surface. Then we get a steady flow because the rigid surface cannot curl up. Then the flow, because of its centrifugal force, exerts on this body a force directed to the left. The magnitude of this so-called suction force is (5)

$$P_x = -\frac{\pi}{4}\varrho\sigma^2. \qquad (34)$$

The negative sign indicates that the force is directed to the left.

If the flow is supposed to be steady, this force can be held only if the surface is rigid. Now we can assume that the circulation distribution according to Equation (3) or (4) is produced, so that we can conceive of this surface as made

(5) See, for instance, R. Grammel, The Hydrodynamic Bases of Flight [Die hydrodynamischen Grundlagen des Fluges], p. 21, Braunschweig, 1917.

up of very many, very small, rotating cylinders, each of which has a circulation $d\Gamma$ such that they exactly yield the total circulation according to Equation (4). Now, if we bend the surface, we displace the individual cylinders in the fluid and, according to a well-known rule of Kutta and Joukowsky (6), this produces forces in the individual cylinders. Now we can think of this bending as being performed so that these forces always exactly compensate for the forces exerted by the total flow on the body and, thus, on the individual cylinders. Then the body no longer experiences any forces. We need no longer consider it to be solid, and can replace it again by the discontinuity surface. Even though we cannot state the necessary motion for every point, we can make a statement about the movement of the center of force, on the basis of the Kutta-Joukowsky rule. According to this rule, the force experienced by a body with the circulation Γ, moving with the velocity w relative to the surrounding fluid, is

$$P = \varrho w \Gamma; \tag{35}$$

It is perpendicular to w.

Now we can also express this rule in such a way that for a change in velocity by the amount w there results a change in force by the amount P, according to Equation (35). In this form, we become independent of the concept of "velocity relative to the surrounding fluid", which is not always easily established. Further, we can also apply the Kutta-Joukowsky rule to a multitude of bodies with circulation. Then the resulting total force is

$$P_y = \varrho \sum \Gamma u, \tag{36}$$

$$P_x = -\varrho \sum \Gamma v. \tag{37}$$

(6) See its presentation in Handbuch der Physik [Handbook of Physics], Volume VII, Chapter 1, Figure 55; Berlin, 1927.

Here, again, we can consider u and v to be velocity changes and P to be the force change.

In our case, with a continuous vortex distribution, the $\Sigma|$ transform into $\int|$. Now we must move the vortex so that the force

$$P_x = -\frac{\pi}{4}\varrho\sigma^2 \Big|$$

disappears and P_y remains unchanged at zero. That is, in the movement we must have

$$\varrho\int v\frac{\partial\Gamma}{\partial s}ds = -\frac{\pi}{4}\varrho\sigma^2 \tag{38}$$

and

$$\varrho\int u\frac{\partial\Gamma}{\partial s}ds = 0 \tag{39}$$

where s is the arc length of the discontinuity surface and the integral is to be extended over the entire length of the discontinuity surface. The velocities u and v are to be calculated relative to the original straight discontinuity surface.

We can also interpret Equations (38) and (39) in still another way: the flow becomes non-steady due to the deformation of the separation surface (curling of the edge). This non-steady character of the flow results in accelerations of the fluid particles, especially in the region of the coiled end which is growing with time, produced by the force according to Equation (34). For the condition that the sum of all the acceleration forces is equal to $\frac{\pi}{4}\varrho\sigma^2\Big|$, we have found an equivalent relation in Equations (38) and (39).

In the later application of this rule, we will consider vortex systems in which vortices transform from one system into the other, so that the circulation of a system under consideration changes. As the usual Joukowsky rule presupposes constant circulation, it is convenient in this case to formulate the center of force rule somewhat differently. We can say: If no force acts, the position of the center of force remains unchanged, or the moment of all vortices for any given reference point is constant. Now if a force P acts, the / 154
center of force shifts corresponding to the Joukowsky rule, or the change of the moment for all vortices and for a given reference point is equal to the force P. Thus, for our case we have

$$\frac{\partial}{\partial t}\int \frac{\partial \Gamma}{\partial s} x\, ds = 0 \qquad (40)$$

and

$$\frac{\partial}{\partial t}\int \frac{\partial \Gamma}{\partial s} y\, ds = P_x. \qquad (41)$$

As for the forces, we can also establish corresponding conditions for the moments of these forces. The forces arising from the vortex displacements according to the Joukowsky rule must be equal to the force P_x not only in magnitude and direction, but also in position. Now, as all the vortices are below the x-axis, the resultant P_x arising from the vertical movement of the vortices is certainly also below the x-axis. In order to compensate for the moment which results, the horizontal displacements of the vortices must produce an equal and opposite moment. As the latter motion produces zero as a resultant force, the position of the center of rotation is immaterial. For instance, we can place it in the coordinate origin and obtain

$$\varrho\int v y \frac{\partial \Gamma}{\partial s} ds = \varrho\int u x \frac{\partial \Gamma}{\partial s} ds. \qquad (42)$$

If the center of force remains unchanged in a system of vortices, then the resultant of the forces arising according to the Joukowsky rule for the individual vortex likewise is zero. But these forces produce a moment if the vortex has an average motion (concentrating) toward the center of force or away from it. For a concentrating movement, the moment is opposite to the direction of rotation of the vortex, and in the same direction for the opposite movement.

If we wish to concentrate a number of vortices Γ_1, Γ_2, at a point, we need a moment of momentum (the moment M must act for the time t)

$$Mt = \tfrac{1}{2} \sum \Gamma_n r_n^2, \tag{43}$$

where r_n indicates the distance of the vortex Γ_n from the point of concentration.

2. First Approximation for the Center of Force of the Spiral Core

From the estimates in Chapters II and III we know that for the spiral we must differentiate two regions — the interior with coils which are to some degree circular, and the exterior, in which the curve asymptotically approaches a straight line. Between the two regions, there is a relatively very short transition section, about which we can say little. We establish a separation between the two regions at the point $\varphi = \frac{\pi}{2}$ (Figure 16) and consider the two regions separately. In the following, we call the internal region with $\varphi \geq \frac{\pi}{2}$ the spiral core.

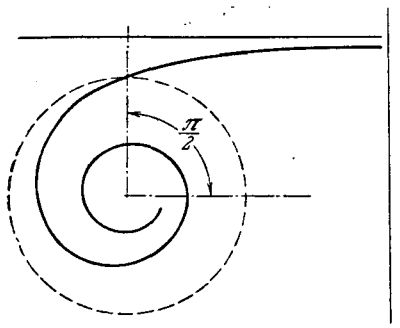

Figure 16. Separation of the spiral core.

In Chapter III we have already emphasized that the process of curling at the edge of the separation surface is equivalent to a concentration of the vortex about the zero point of the spiral. The approximately circular coils of the spiral core form a system of vortices which is to some extent circularly symmetrical, having a field which at some distance differs only slightly from that of a single vortex at the center of force of the core. Thus, for evaluation of the action toward the outside, we can think of the inner part of the discontinuity surface

$\left(\varphi > \frac{\pi}{2}\right)$ as a single vortex with circulation Γ_0 concentrated / 155
at the center of force. Here Γ_0 is the circulation about the part of the discontinuity surface inside the point $\varphi = \frac{\pi}{2}$ (inside the dashed circle in Figure 16). Let the point $\varphi = \frac{\pi}{2}$ of the spiral have the distance X_0 from the edge of the discontinuity surface before curling, so that

$$\Gamma_0 = 2\sigma\sqrt{X_0}$$

In the first approximation, the values of which we designate in the following by the index 1, we obtain the action of the concentration if we concentrate into one point the vortex elements which lie on the segment X_0 from the starting point and at first consider the vortex of the remaining segment to be undisturbed.

Because of the asymmetry due to the arbitrary separation of the spiral core at the point $\varphi = \frac{\pi}{2}$, the center of force for the vortex of the core does not coincide with the center of the spiral. To differentiate from the coordinates a and b of the center, we shall designate the coordinates of the center of force as a' and b' (see Figure 19).

As the center of force for the vortex cannot shift in the x-direction, the abscissa a' for the center of force of the core must coincide with the center of force of the original

vortex segment from Q to X_0. Therefore, $a'_1 = 1/3\ X_0$. In the analogous enlargement, X_0 grows according to the time formula

$$X_0 = x_0 t^{\frac{2}{3}}; \tag{44}$$

thus, we have also

$$a'_1 = \tfrac{1}{3} X_0 = \tfrac{1}{3} x_0 t^{\frac{2}{3}}. \tag{45}$$

The quantity x_0 is related to the quantity σ defined by Equation (4). In the following we must explain this relation more accurately The movement of the core center of force in the x-direction, in relation to the original discontinuity surface, thus occurs with a velocity

$$U_1 = \frac{\partial a'_1}{\partial t} = \frac{2}{9} \frac{x_0}{t^{\frac{1}{3}}} = \frac{2}{9} \frac{X_0}{t} \tag{46}$$

For the separation b'_1 of the center of force from the x-axis, or for the rate of migration in the vertical direction $V_1 = \left|\frac{\partial b'_1}{\partial t}\right|$, we obtain from the Joukowsky relation (Equation (38) and adjacent comments)

$$P_x = -\varrho \frac{\pi}{4} \sigma^2 = \frac{\partial}{\partial t} (\varrho \Gamma_0 b'_1) = \varrho \Gamma_0 V_1 + \varrho b'_1 \frac{\partial \Gamma_0}{\partial t} = \varrho V_1 \cdot 2\sigma \sqrt{X_0} + \frac{2}{3} \varrho \sigma \frac{\sqrt{X_0}}{t} b'_1;$$

but since

$$\frac{2}{3} \frac{b'_1}{t} = \frac{\partial b'_1}{\partial t} = V_1$$

then V_1 becomes

$$V_1 = -\frac{\pi\sigma}{12\sqrt{X_0}} = -\frac{\pi\sigma}{12\sqrt{x_0}} t^{-\frac{1}{3}} \tag{47}$$

and

$$b'_1 = \int_0^t V_1 dt = -\frac{\pi\sigma}{8\sqrt{x_0}} t^{\frac{2}{3}} = -\frac{\pi\sigma}{8 x_0^{\frac{3}{2}}} X_0. \tag{48}$$

The negative sign means that the center of force is below the X-axis. Of course, these relations apply only approximately, as we have at first neglected the movements of the outer part of the discontinuity surface. But since we can with this know approximately the location of the vortex filament at any time (except, at first, for the constant $\sigma/x_0^{\frac{3}{4}}$), we can also calculate approximately the perturbation velocities u and v along the outer part of the vortex segment, on the basis of Equations (26) to (28). But now the resulting shifts of the vortex for the outer part of the spiral make necessary a correction of our calculation of the position of the center of the spiral, on the basis of the center of force rule [Equations (38) and (39)]. The new position of the center then produces somewhat different shifts in the outer part, etc. / 156

3. The Time Constant

Before we calculate these further approximations, however, we must know something more of the constant $\sigma/x_0^{\frac{3}{4}}$. This is, on one hand, a measure for the rate of the coiling process, and on the other hand it has an important relation to the dimensions of the core.

So far, we have considered the spiral core as concentrated in its center of force. This is of no importance for the calculation of its flow field or for determination of the resultant forces due to the movement of the center of force. But we have already noted, in the explanation of the center of force rule, that a moment is necessary for concentration of vortices. Thus, for the calculation of the moments it is no longer a matter of indifference what radius the spiral core has. So we can expect, from the condition that no moment acts on the discontinuity surface, a statement about the dimensions of the spiral core, and particularly on the factor $\varkappa$ characterizing these dimensions in Equation (9).

The shift of the core center of force produces a moment which is exactly compensated by the movement of the other vortices, particularly through their approach to the spiral core. But this movement of the other vortices occurs under the influence of the spiral core. It is determined essentially only by the position of its center of force and hardly at all by the distribution of the vortices [7]. So we can consider the state at time t to have arisen in this way: we concentrate the vortices of one segment x in their center of force, then shift them toward the spiral core center of force, simultaneously allowing the other vortices to move toward their final positions, and finally redistributing the vortices concentrated in the core center of force in correspondence with the distribution in the spiral core. In this, we need not consider the entire spiral core, but can limit ourselves, for example, to only the inner part of it. The moment produced by the shift of the vortices concentrated in their center of force is compensated by the simultaneous migration of the other vortices. Thus, so that no moment of momentum remains in the fluid, the moment of momentum resulting from the concentration of the vortex must be equally opposed by the moment of momentum due to distribution of the concentrated vortex.

In order to concentrate into their center of force at 1/3 x_1 the vortices on the segment from 0 to x_1, with a total strength $\Gamma_1 = 2\sigma\sqrt{x_1}$ distributed according to the function

$$\Gamma' = \frac{\partial \Gamma}{\partial x} = \frac{\sigma}{\sqrt{x}}$$

a moment of momentum

$$(Mt)_1 = \varrho \int_0^{x_1} \Gamma' \frac{x^2}{2} dx - \frac{\varrho}{2} \Gamma_1 \left(\frac{x_1}{3}\right)^2 = \frac{2}{45} \varrho \Gamma_1 x_1^2 \qquad (49)$$

(7) As this requirement is not exactly met, the following calculation represents only the first stage of an approximation procedure. But it appears, if we test this requirement on the basis of the later results, that the difference of about 1% is within the range of calculating accuracy. It remains, therefore, to calculate more approximations for κ.

is necessary. (The moment M must be exerted during the time t / 157 in order to effect the shift.)

In order to distribute this vortex in the core over a circle with radius r_1 according to the function

$$\Gamma' = \frac{\partial \Gamma}{\partial r} = \frac{\varkappa}{\sqrt{r}}$$

it is necessary to have an opposite moment of momentum

$$(Mt)_2 = \varrho \int_0^{r_1} \Gamma' \frac{r^2}{2} = \frac{1}{10} \varrho \Gamma_1 r_1^2 \qquad (50)$$

These two moments of momentum must be equal, according to the above. This gives

$$\frac{r_1^2}{10} = \frac{2}{45} x_1^2$$

or

$$r_1 = \tfrac{2}{3} x_1. \qquad (51)$$

As the vortices distributed on the circular surface r_1 have the total strength

$$\Gamma_1 = 2\varkappa \sqrt{r_1} = 2\sigma \sqrt{x_1} \qquad (52)$$

we obtain

$$\varkappa = \sigma \sqrt{\frac{x_1}{r_1}} = \sqrt{\frac{3}{2}}\sigma. \qquad (53)$$

With the quantity $\varkappa$ now, not only is the constant determining the size and shape of the core given, but also some evidence on the speed of the process (time constant). We can express this rate somewhat if we state the segment x_0 of the original discontinuity surface which has, after the passage of the time unit, moved just to the edge of the spiral core. This distance depends, obviously, on the intensity of the

discontinuity surface, which is expressed by σ. If we use the equation

$$r = \left(\frac{\varkappa t}{\pi\varphi}\right)^{\frac{2}{3}}$$

for the spiral core out to the point $\varphi = \frac{\pi}{2}$, and so ignore the small deviation near the edge of the core, then for $t = 1$ and $\varphi = \frac{\pi}{2}$ we obtain

$$x_0 = \frac{3}{2} r_0 = \frac{3}{2}\left(\frac{2\varkappa}{\pi^2}\right)^{\frac{2}{3}} = \left(\frac{3}{2}\right)^{\frac{4}{3}}\left(\frac{2\sigma}{\pi^2}\right)^{\frac{2}{3}},$$

and, therefore,

$$\frac{x_0}{\sigma^{\frac{2}{3}}} = \left(\frac{9}{2\pi^2}\right)^{\frac{2}{3}} \quad \text{or} \quad \frac{\sigma}{x_0^{\frac{3}{2}}} = \frac{2}{9}\pi^2. \tag{54}$$

So we have now all the important quantities so that we can state the shape of the spiral at some time t, expressed by the constant $\sigma = \frac{\Gamma}{2\sqrt{\varkappa}}$ of the original discontinuity surface.

4. More Accurate Calculation of the Core Center of Force

With this more accurate knowledge of the rate of the coiling process, we can pursue further the determination of the movement of the core center of force, which we started earlier. The factor $\sigma/x_0^{\frac{3}{2}}$ appeared [Equation (48)] in the determination of the vertical distance b' of the center of force from the original discontinuity surface. Now that we know the relation between x_0 and σ from Equation (54) $\left(\frac{\sigma}{x_0^{\frac{3}{2}}} = \frac{2}{9}\pi^2\right)$, we obtain from Equation (48) / 158

$$b_1' = -\frac{\pi}{8}\frac{\sigma}{x_0^{\frac{3}{2}}} X_0 = -\frac{\pi^3}{36} X_0. \tag{55}$$

With this value and the value $a'_1 = 1/3\ X_0$ [Equation (46)] we can now calculate further approximations for a' and b'.

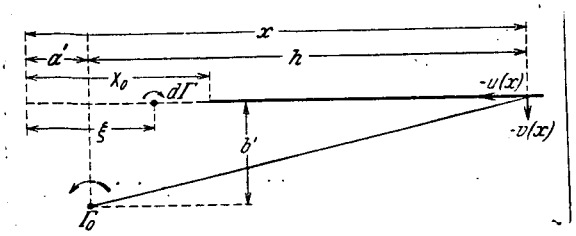

Figure 17

We obtain the effect of the vortex concentration by the method in Chapter III, through superposition of double vortices on the original vortex system, which was previously in equilibrium. Thus, we obtain the perturbation velocity $v_1(x)$ for the vertical component at a point x on the vortex segment according to Figure 17:

$$v_1(x) = -\frac{1}{2\pi}\int_0^{X_0} \frac{\Gamma'(\xi)\,d\xi}{x-\xi} + \frac{\Gamma_0}{2\pi}\,\frac{x-a_1'}{(x-a_1')^2+b_1'^2}.$$

With

$$b_1' = -\frac{\pi}{8}\,\frac{\sigma}{x_0^{\frac{3}{2}}}X_0, \quad \Gamma' = \frac{\sigma}{\sqrt{\xi}}, \quad \Gamma_0 = 2\sigma\sqrt{X_0} \quad \text{and} \quad a_1' = \tfrac{1}{3}X_0$$

we get, after performing the integration

$$v_1(x) = -\frac{\sigma}{\pi}\left\{\frac{1}{2\sqrt{x}}\ln\frac{1+\sqrt{\frac{X_0}{x}}}{1-\sqrt{\frac{X_0}{x}}} - \frac{\sqrt{X_0}}{\left(x-\frac{1}{3}X_0\right)\left(1+\frac{b_1'^2}{\left(x-\frac{1}{3}X_0\right)^2}\right)}\right\}. \qquad (56)$$

On the basis of the law of analogous enlargement of the spiral with time [Equation (6)] we can calculate the time course of v for a given position x from the distribution of v along x or ξ at a given time t_1. In this way we can determine the shift of a point in the y-direction

$$y(x) = \int_0^{t_1} v(t)\,dt = \frac{3}{2}t_1 x\int_x^{\infty}\frac{v(\xi)}{\xi^2}\,d\xi. \qquad (57)$$

If we carry out this calculation for the function v(x) above, we obtain

$$\frac{y(x)}{X_0} = -\frac{3}{2}\,\frac{\sigma}{\pi x_0^{\frac{3}{2}}}z\left[\frac{2}{3z^{\frac{3}{2}}}\operatorname{Arc\,Tg}\frac{1}{\sqrt{z}} + \frac{1}{6}\left\{\frac{1}{z} + \ln\left(1-\frac{1}{z}\right)\right\}\right. \qquad (58)$$

$$-\frac{1}{\left(\frac{b'}{X_0}\right)^2+\frac{1}{9}}\left\{\frac{\left(\frac{b'}{X_0}\right)^2-\frac{1}{9}}{\left(\frac{b'}{X_0}\right)^2+\frac{1}{9}}\ln\frac{\sqrt{\left(z-\frac{1}{3}\right)^2+\left(\frac{b'}{X_0}\right)^2}}{z}\right.$$

$$\left.-\frac{1}{3z}-\frac{2}{3}\frac{\frac{b'}{X_0}}{\left(\frac{b'}{X_0}\right)^2+\frac{1}{9}}\left[\frac{\pi}{2}+\operatorname{arc\,tg}\frac{z-\frac{1}{3}}{\frac{b'}{X_0}}\right]\right\}, \qquad (58)$$

in which, for brevity, we have set $x/X_0 = z$.

We can plot the shape and position of the spiral core approximately on the basis of the first approximation. / 159
To be sure, we also need the previously mentioned difference between the center of force coordinates a', b' and the center coordinates a,b. The calculation can be performed rather easily if we assume, for an approximate determination, that the exponent ν (Equation (12)) increases by 2/3 up to the edge of the core. If we designate the radius of the core as R_0 and set $R_0 = 2/3\ X_0$, following Equation (51), then for the position of the center of force we get (Figure 19)

$$\left.\begin{aligned} a-a' &= \Delta a = \quad 0{,}15\,R_0 = \quad 0{,}10\,X_0, \\ b-b' &= \Delta b = -0{,}07\,R_0 = -0{,}05\,X_0. \end{aligned}\right\} \qquad (59)$$

If we draw the spiral core approximately with these values and attempt to plot the outer part of the spiral in this figure on the basis of Equation (58), we see that the y-values which we have obtained are considerably too large in the vicinity of the core, so that the curve we obtain does not connect to the edge of the core. This is because our calculation is allowable only for large x. Now we can proceed, drawing the curve for the outer spiral by eye, so that it transforms gradually from the edge of the spiral core in a smooth curve into the calculated curve. At first glance, to be sure, this process seems very inaccurate, especially because in this case a satisfactory transition occurs only at rather high x-values. But since y is already rather small at the edge of the spiral, and quickly moves to considerably smaller values (cf. Figure 19), accurate knowledge of the course of the curve is not really necessary.

We do need to know the curve to find the position of the force center of the core. If b'_2 is the second approximation for b', then

$$\Gamma_0(b'_1 - b'_2) = \int_{X_0}^{\infty} \Gamma' y \, dx. \tag{60}$$

If we perform this calculation with the values of y taken partly from the drawing and partly from the calculation, we get

$$\begin{aligned} b'_1 - b'_2 &= 0{,}04\, b'_1, \\ b'_2 &= 0{,}96\, b'_1 = -\frac{\pi^3}{36} \cdot 0{,}96 \cdot X_0 = -0{,}83\, X_0. \end{aligned} \tag{61}$$

This second approximation differs so little from the first one that it is not worth while to seek more improvement of this value. We also see that the somewhat uncertain determination of the y-value is rather unimportant because of the smallness of the correction to the result.

We can set up a completely corresponding calculation for the velocity u and the resulting shifts Δx in the x-direction. For sufficiently large x,

$$u(h) = \frac{\Gamma_0}{2\pi} \frac{b'_1}{b'^2_1 + h^2}, \tag{62}$$

where $h = x - a'_1$. In the same way as for the y-component, we get from $u(x)$ the time course of $u = u(t)$ for a given x, and from that we obtain the displacement

$$\Delta x = \int_0^t u(t)\, dt = \frac{3}{2} t_1 x \int_x^{\infty} u(\xi) \frac{d\xi}{\xi^2}. \tag{63}$$

Performance of the calculation yields, in correspondence to that for the vertical displacement [Equation (58)]: / 160

$$\begin{aligned} \frac{\Delta x}{X_0} = \frac{3}{2} \frac{\sigma}{\pi} \frac{1}{x_0^{\frac{3}{2}}} z \Bigg\{ & \frac{2}{3} \frac{\frac{b'}{X_0}}{\left[\left(\frac{b'}{X_0}\right)^2 + \frac{1}{9}\right]^2} \ln \frac{\sqrt{\left(\frac{b'}{X_0}\right)^2 + \left(z - \frac{1}{3}\right)^2}}{z} \\ & + \frac{\left(\frac{b'}{X_0}\right)^2 - \frac{1}{9}}{\left[\left(\frac{b'}{X_0}\right)^2 + \frac{1}{9}\right]^2} \left(\frac{\pi}{2} + \operatorname{arc\,tg} \frac{z - \frac{1}{3}}{\frac{b'}{X_0}} \right) + \frac{\frac{b'}{X_0}}{\left(\frac{b'}{X_0}\right)^2 + \frac{1}{9}} \frac{1}{z} \Bigg\}. \end{aligned} \tag{64}$$

For the point $x = X_0$ we have again the condition that it must move directly toward the core boundary. That is, it is necessary for it that $\Delta x = a_1' + \Delta a - X_0 = -0{,}57\, X_0$. (For Δa, see Equation (59)). The value of Δx calculated from the formula above for $z = 1$ or $x = X_0$ is considerably smaller, namely $-0.305\, X_0$. For this reason, we will here again first correct the curve for Δx by eye so that it takes on the magnitude $-0.57\, X_0$ for $z = 1$. With the values for Δx found in this way, we can correct the abscissa a' so that

$$\Gamma_0 (a_2' - a_1') = -\int_{X_0}^{\infty} \Gamma' \Delta x \, dx \qquad (65)$$

From this we get

$$a_2' \approx 1{,}54\, a_1'. \qquad (66)$$

Now this difference of a_2' and a_1' is not as insignificant as that of b'_2 and b'_1. Thus, we must calculate still a third approximation. A considerable inaccuracy of the latter calculation is in the fact that we calculated the velocities u(x) for the positions x of the original discontinuity surface, while in reality the vortex elements concerned have been shifted by y and Δx to another position. If, in Equation (62) we insert instead of b'_1, a'_1, and x the improved values $b'_2 - y$, a'_2, and $x - \Delta x$, and carry out the calculation otherwise in the same way, then for the point $x = X_0$ we get a shift $\Delta x = -0.45\, X_0$, while the value given geometrically is $\Delta x = -(X_0 - a_2' - \Delta a) = -0{,}39\, X_0$. Accordingly, a'_3 becomes 1.38 a'_1.

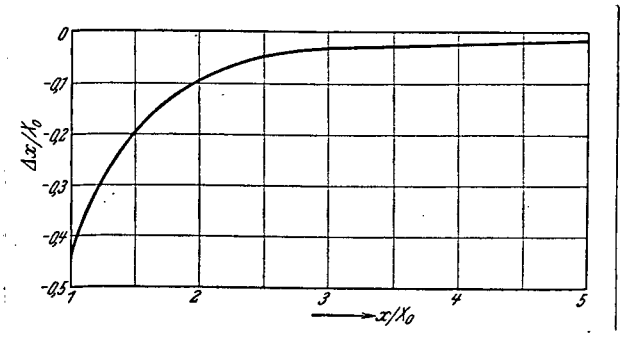

Figure 18. Vortex shift in the x-direction.

Another repetition of the process gives $\Delta x = -0.44\, X_0$ both from the calculation and from the geometric relation. The resulting curve for Δx is shown in Figure 18. According to this, a'_4 becomes

$$a_4' = 1{,}41\, a_1' = 0{,}47\, X_0. \qquad (67)$$

The difference between a'_3 and a'_4 is again satisfactorily small, so that more approximations are unnecessary. For the midpoint of the spiral, which is away from the center of force by the amount $\Delta a| = 0.10\ X_0$ or $\Delta b| = -0.05\ X_0$ [Equation (59)] we obtain the coordinates

$$\left.\begin{aligned} a &= a' + \Delta a = \quad 0{,}57\, X_0, \\ b &= b' + \Delta b = -0{,}88\, X_0. \end{aligned}\right\} \qquad (68)$$

In calculation of the velocity v and the resulting displacement y we have limited ourselves to the first approximation in Equation (57) and (58), as it appeared that these quantities were only of quite insignificant effect on the calculation of the distance of the center of force, b. But in fact the shifts $\Delta x|$ make a relatively large contribution for v and y. For completeness, we shall calculate a second approximation of the matching y-values, at least for very large x. In the first approximation [Equation (58)] the simplified relation / 161

$$y_1 = -X_0 \frac{0{,}217}{\left(\frac{x}{X_0}\right)^3}.$$

appears for large x. According to Equation (29), the effect of a displacement $\Delta\xi|$ of a vortex $\Gamma'(\xi)d\xi|$ at point $\xi|$ and a simultaneous opposite displacement of the spiral core to maintain the position of the center of force on the velocity v at point x is

$$dv = \frac{\Delta\xi}{2\pi} \frac{2\left(\xi - \frac{X_0}{3}\right)}{x^3} \frac{\sigma}{\sqrt{\xi}} d\xi,$$

in which $\xi_1 = \xi,\ \xi_2 = \frac{X_0}{3}|$ and $d\Gamma(\xi_1) = \Gamma'(\xi)d\xi = \frac{\sigma}{\sqrt{\xi}}\, d\xi|$. If, for $\Delta\xi|$ we insert the value from Figure 18, then by integration we get

$$v_2 - v_1 = -0{,}91\, v_1$$

and, further

$$\left.\begin{aligned} y_2 - y_1 &= -0{,}91\, y_1, \\ y_2 &= -X_0 \frac{0{,}42}{\left(\frac{x}{X_0}\right)^3}. \end{aligned}\right| \qquad (69)$$

According to Equation (64), the shift in the x-direction for very large x is

$$\left.\Delta x = -X_0 \frac{0{,}29}{\left(\frac{x}{X_0}\right)^2}.\right| \qquad (70)$$

5. Summary

Thus, we now have all the quantities which are important for the shape of the spiral and the time course of its growth. For review, we combine the most important formulas with the constants:

Original discontinuity surface:

$$\left.\Gamma = 2\sigma\sqrt{x};\right| \qquad \left|\sigma\right| = \text{given constant} \qquad (4)$$

Shape of the spiral in the interior:

$$\left.\begin{aligned} r &= \left(\frac{\varkappa t}{\pi\varphi}\right)^{\frac{2}{3}}; \\ \Gamma &= 2\varkappa\sqrt{r}. \end{aligned}\right| \qquad \left|\varkappa = \sqrt{\tfrac{3}{2}}\sigma\right| \qquad (11) \qquad (53)$$

Shape of the spiral at a great distance:

Displacement of a point

$$\left.\begin{aligned} y &= -\frac{0{,}42}{\left(\frac{x}{X_0}\right)^3} X_0, \\ \Delta x &= -\frac{0{,}29}{\left(\frac{x}{X_0}\right)^2} X_0. \end{aligned}\right| \qquad \begin{matrix} (69) \\ (70) \end{matrix}$$

Rate of coiling:

After the time $t = 1$, a point x_0 of the original discontinuity surface has moved just to the edge of the spiral core $\left(\varphi = \frac{\pi}{2}\right)$. We have

$$x_0 = \left(\frac{9}{2\pi^2}\sigma\right)^{\frac{2}{3}}. \qquad (54)$$

After the time t, a point X_0 of the original discontinuity surface has moved to the edge of the spiral core. According to Equations (44) and (54), we have / 162

$$X_0 = x_0 t^{\frac{2}{3}} = \left(\frac{9}{2\pi^2}\sigma t\right)^{\frac{2}{3}}. \qquad (71)$$

Coordinates of the coil center point:

$$a = 0{,}57\, X_0, \qquad (68)$$

$$b = -0{,}88\, X_0, \qquad (61)$$

$$\alpha = \operatorname{arc\,tg}\frac{b}{a} = -57^0. \qquad (72)$$

The form of the spiral resulting from this is shown in Figure 19.

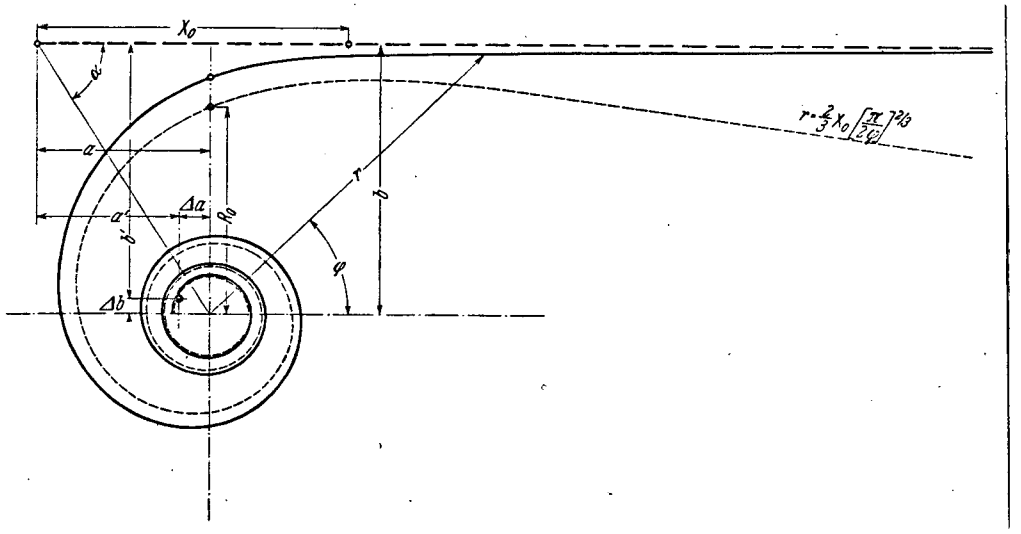

Figure 19. Form of the spiral.

V. APPLICATIONS TO AIRFOIL WING THEORY

1. Wing With Finite Span

In order to relate to the problem mentioned in the introduction, we should investigate somewhat the vortex surface behind a wing with finite span, so that we can at least approximately apply the results we have obtained to the practical case.

For an airfoil, the lift is approximated by an ellipse across the span width. If $\Gamma_{\max}$ is the circulation in the center of the wing and L is the span of the wing, then the circulation at a distance z from the middle is

$$\Gamma = \Gamma_{\max} \sqrt{1 - \left(\frac{2z}{L}\right)^2}. \tag{73}$$

According to well-known laws of airfoil theory [8] this circulation about the wing at point z is equal to the circulation about the segment of the discontinuity surface behind the wing from the edge to point z. The last equation at the same time shows the distribution of the circulation in the discontinuity surface. If we set the distance from the edge $\frac{L}{2} - z = x$ or $1 - \frac{2z}{L} = \frac{2x}{L}$, then near the edge we get

$$\Gamma \approx 2\Gamma_{\max} \sqrt{\frac{x}{L}}. \tag{74}$$

With our theoretical calculation we had

$$\Gamma = 2\sigma\sqrt{x}.$$

Thus, we have

$$\sigma = \frac{\Gamma_{\max}}{\sqrt{L}}. \tag{75}$$

---

(8) Cf. Handb. d. Physik [Handbook of Physics] Vol. VII, Chapter 4, Figure 27.

According to the well-known laws of airfoil wing theory[9] the velocity at which the uncurled discontinuity surface advances is

$$w_0 = \frac{\Gamma_{max}}{L}; \tag{76}$$

so that

$$\sigma = w_0 \sqrt{L}. \tag{77}$$

Now the process of coiling both ends of the discontinuity surface occurs until the circulation of one coil core has grown to the maximum circulation Γ_{max}. Then the original plane vortex surface has transformed into two separate vortices with the circulation $\pm \Gamma_{max}$.

The separation L' of the midpoints of these two vortices arises from the condition that the midpoint of a vortex must have the same horizontal distance from the center of the wing as the center of force for the vortex of one half of the discontinuity surface. It is

$$L' = \frac{\pi}{4} L. \tag{78}$$

The velocity with which the two vortices move is

$$w_0' = \frac{\Gamma_{max}}{2\pi L'} = \frac{2}{\pi^2} \frac{\Gamma_{max}}{L} = \frac{2}{\pi^2} w_0. \tag{79}$$

The velocity of the flow in the middle between the two vortices, which was w_0 before the coiling, has dropped to

$$w_0^* = \frac{2\Gamma_{max}}{2\pi \frac{L'}{2}} = \frac{8}{\pi^2} w_0 \tag{80}$$

after coiling.

---

(9) Cf. Handb. d. Physik [Handbook of Physics], Vol. VII, Chapter 4, Figure 31.

2. The Coiling Time

For practical application, it is now important to answer the question: at what distance from the trailing edge of the wing can we consider the process of coiling to be finished? This distance cannot be determined exactly, of course, as an asymptotic transition to the final state takes place. But we can help ourselves by replacing the asymptotic transition with a discontinuous one (Figure 20). We continue the movement which, according to the theory, is valid for the beginning, until the center of the coil is so far from the end of the wing that it corresponds to the final state of the single vortex (point S, Figure 20). From there on, the movement of the vortex couple is supposed to proceed according to its laws. Now we define as the coiling time, T, that time which is needed, under the assumption given, to reach the point S. For this time, according to Equations (68) and (71), we have

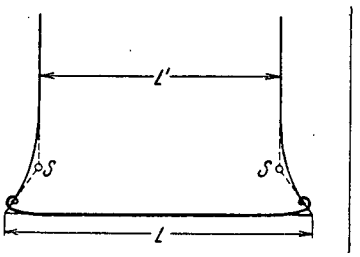

Figure 20. Vortex movement behind a wing of finite span width.

$$\frac{L-L'}{2}=0{,}57\left(\frac{9\sigma}{2\pi^2}T\right)^{\frac{2}{3}}.$$

$$T=\frac{2\pi^2}{9\sigma}\left(\frac{L-L'}{1{,}14}\right)^{\frac{3}{2}}=\frac{2\pi^2}{9w_0\sqrt{L}}\left(\frac{L\left(1-\frac{\pi}{4}\right)}{1{,}14}\right)^{\frac{3}{2}}=0{,}057\frac{L}{w_0}=0{,}057\frac{L^2}{\Gamma_{\max}}. \qquad (81)$$

In this time, the wing passes through the distance / 164

$$E=V_0T=0{,}057\frac{V_0L^2}{\Gamma_{\max}} \qquad (82)$$

if the flight velocity is V_0.

As the total lift of the wing is

$$A=\frac{\pi}{4}\varrho L V_0\Gamma_{\max}$$

with this value we get the relation

$$\frac{E}{L}=0{,}057\frac{\pi}{4}\varrho\frac{V_0^2L^2}{A}=0{,}045\varrho\frac{V_0^2L^2}{A}. \qquad (83)$$

We can also introduce the lift coefficient

$$c_a = \frac{A}{\frac{\rho}{2} F V_0^2},$$

in which F is the greatest projection of the wing (as a rule, span width times wing chord). Then from (82) we get

$$\frac{E}{L} = 0{,}090 \frac{L^2}{F c_a}. \qquad (84)$$

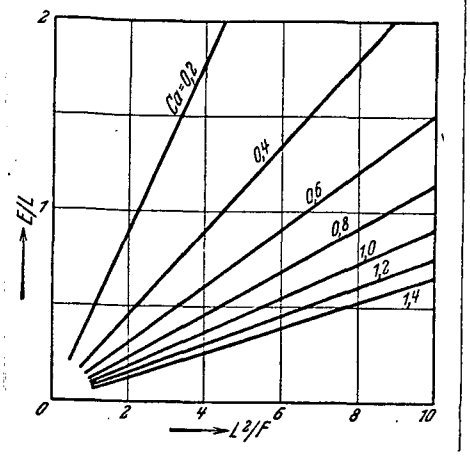

Figure 21. Ending of the curling behind a wing.

This formula states how the ratio of the characteristic distance E to the span width L at given c_a depends on the aspect ratio L^2/F for the wing. Figure 21 shows a graphic presentation of this dependence. Thus, the rolling up is completed relatively near the wing at the larger values of c_a and at moderate aspect ratios.

VI. COMPARISON WITH EXPERIMENT

1. Experimental Arrangement

There are great difficulties on following the curling process experimentally. For one thing, the case of the discontinuity surface which extends to infinity at one side cannot be realized in the experiment. We can only realize the discontinuity surface behind a wing of finite span, or the processes which are approximately described by the results in the previous chapter. Then, only the first stages of these processes are available for comparison with theory. These, because of the small extent of the vortex at the beginning of the movement, are known only with relative inaccuracy. To this major problem we also add the technical one of the experiment, that it is very difficult to obtain these processes to some degree free of incidental motions which

conceal the processes [10]. In spite of this uncertainty it appeared necessary to compare with an experiment, as almost nothing had been known of the course of these processes, so that even a confirmation of the theoretical results to an order of magnitude would be important.

The system used for the experimental investigation is shown in Figure 22. In a long water basin 60 cm wide, a plate, P1, 15 cm wide, perpendicular to the surface of the water, was moved obliquely downward. The slope of the path with respect to the water surface was about 79°, so that the angle of incidence for the plate with respect to the path was some 11°. Seventeen centimeters below the water surface there was a sub-floor B with a slot into which the plate disappeared as it moved. The plate was 21.5 cm long, and reached below the sub-floor even in its highest position. Below the sub-floor, it was connected to a carriage W running on a guide rail. The drive was accomplished in this way: The carriage and the plate were first pulled up by a cord wound on a roller R. The roller could be turned by an electric motor with an intermediate worm gear speed-reducing drive. When the motor was turned on, it unwound the cord from the roller, and the carriage with the plate sank under its own weight with constant velocity. The plate moved at a velocity of about 1.2 m/sec. Before beginning to move, the plate projected about 1 cm above the water surface. By the time the trailing edge entered the water, a fairly constant velocity had been attained. Motion of the water behind the plate as it continued to move downward could be visualized on the water surface by scattered aluminum powder, and recorded by motion pictures. In order to be able to detect particularly the deformation of the vortex layer proceeding from the trailing edge of the plate, the trailing edge was coated with moistened aluminum powder, which floated off when the trailing edge entered the water, and

/ 165

(10) Probably one would get better results if the experiment could be performed on a considerably larger scale than was possible here.

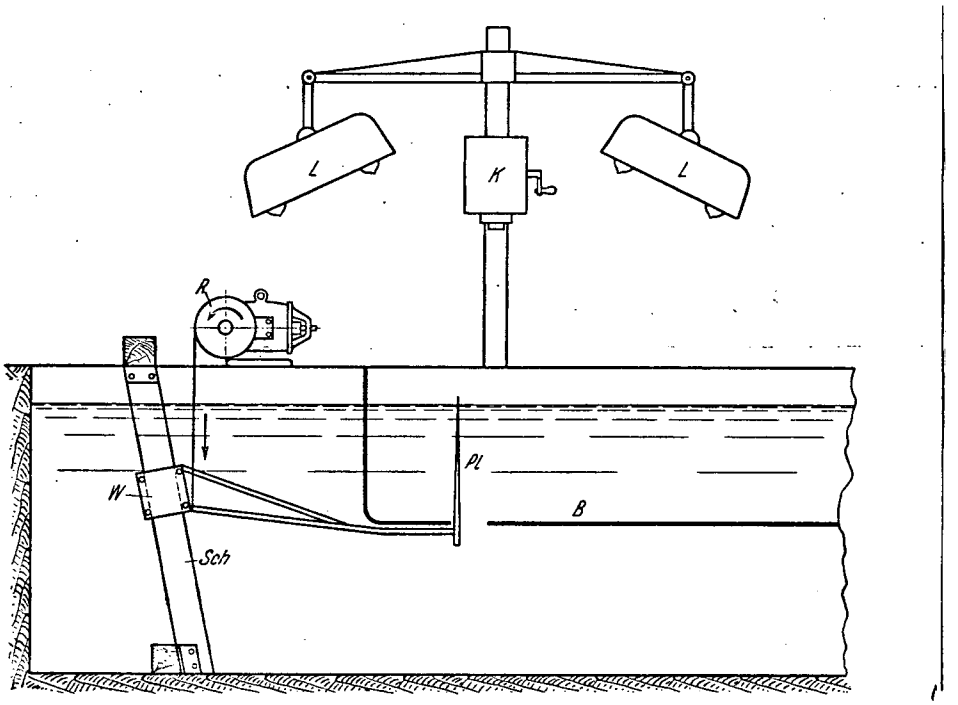

Figure 22. Test system. Pl: plate; B: sub-floor; Sch: guide rail; W: carriage; R: drive roller; L: lamps; K: motion picture camera.

characterized the discontinuity surface. But here there arose the problem that this aluminum powder caused uneven capillary forces on the water surface shortly after floating off. These produced marked characteristic motions of the aluminum particles (see the jagged appearance of the aluminum marking on the first pictures of Figure 23).

2. Experimental Results

The motion picture camera made 16 photographs per second. A selection of these is shown in Figure 23 (every fifth picture in the region of primary interest). In order to be able to measure the photographs more easily, wires were stretched / 167 across the water surface as fixed coordinates. These appear on all the pictures. One wire is transverse to the direction

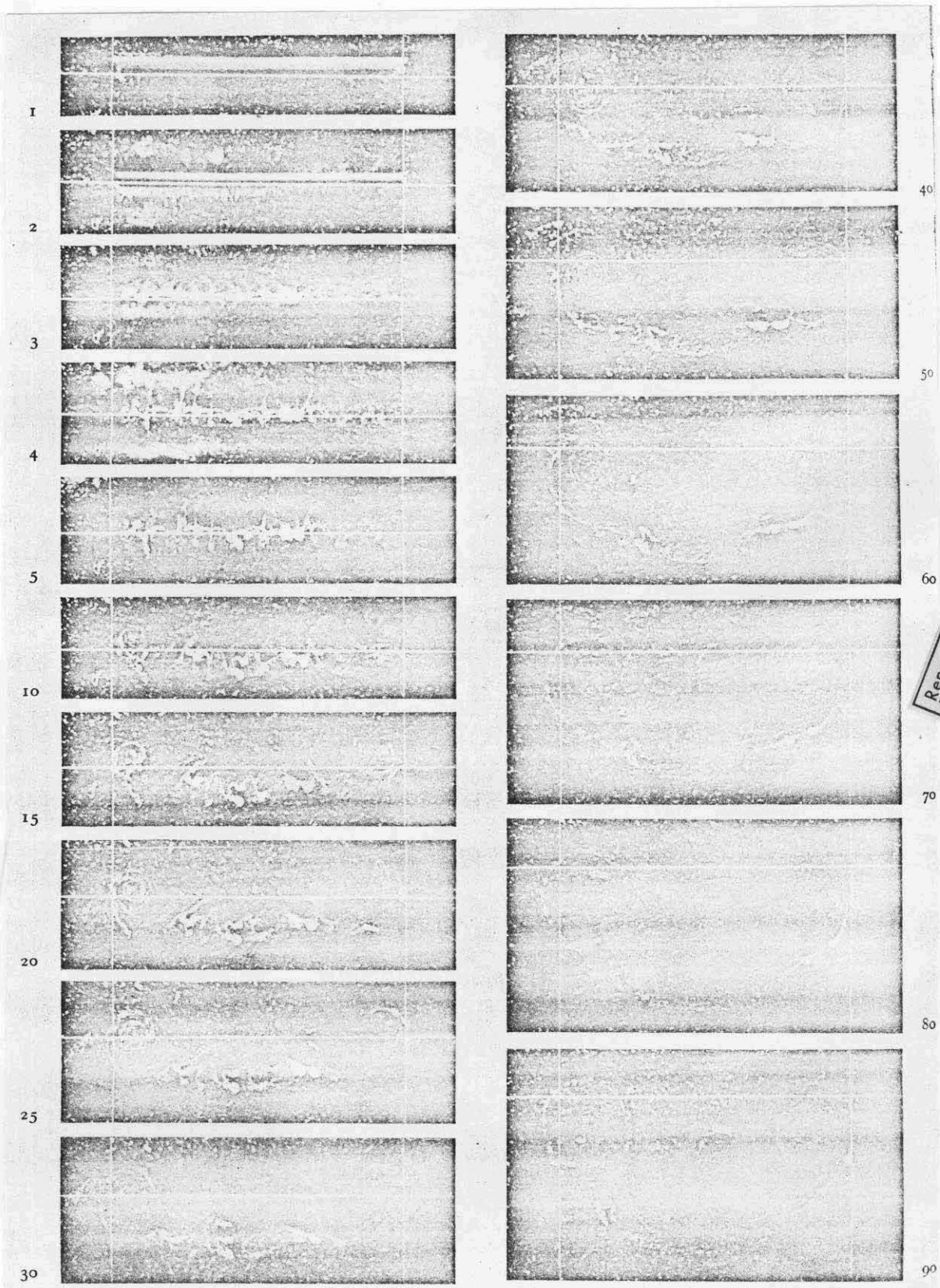

Figure 23. Motion picture frames of the curling process. The numbers indicate the number of the frame (time scale).

of movement approximately at the place where the trailing edge of the plate dips into the water. Two more parallel wires run in the direction of movement, passing approximately through the lateral borders of the plate. The motion of the vortex midpoint was used for comparison with the theory [coordinates a and b in Equation (68)]. The quantity σ appearing in the theory can be determined according to Equation (77) from the motion of the discontinuity surface (velocity w_0).

Measurement of the pictures offered a problem, to the extent that neither the zero point in time nor the zero point of the coordinates could be established exactly. While the zero point in time (immersion of the plate trailing edge) could be determined with some accuracy from the pictures (between frames 2 and 3), the zero point for the coordinates is considerably harder to determine. On one hand, the marking immediately after immersion becomes rather blurred. On the other hand, some flow around the plate and slight vortex formation takes place even before immersion. One must estimate this zero point so that the measured values can be extrapolated freely toward this zero point.

According to Equation (71),

$$X_0 = \left(\frac{9}{2\pi^2}\sigma t\right)^{\frac{2}{3}},$$

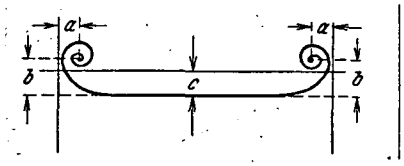

Figure 24

and from Equation (77)

$$\sigma = w_0\sqrt{L}.$$

If we insert the latter value into the previous equation for X_0, noting that $w_0 t = c$ is the displacement of the discontinuity surface (Figure 24), we obtain

$$\frac{X_0}{L} = \left(\frac{9}{2\pi^2}\frac{c}{L}\right)^{\frac{2}{3}}.$$

and so, from Equation (68)

$$\frac{a}{L} = 0{,}57\,\frac{X_0}{L} = 0{,}34\left(\frac{c}{L}\right)^{\frac{2}{3}},$$
$$\frac{b}{L} = 0{,}88\,\frac{X_0}{L} = 0{,}52\left(\frac{c}{L}\right)^{\frac{2}{3}}.$$

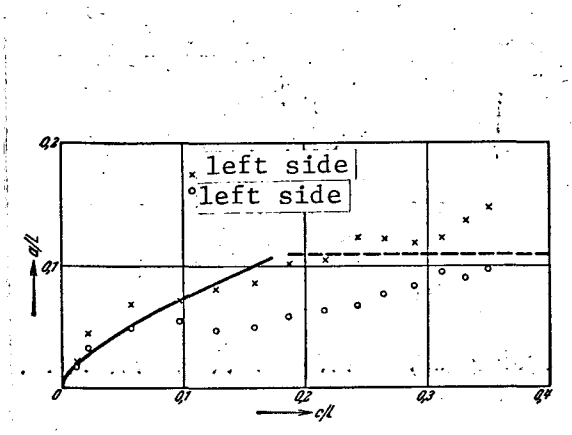

Figure 25. Movement of the vortex in the horizontal direction.

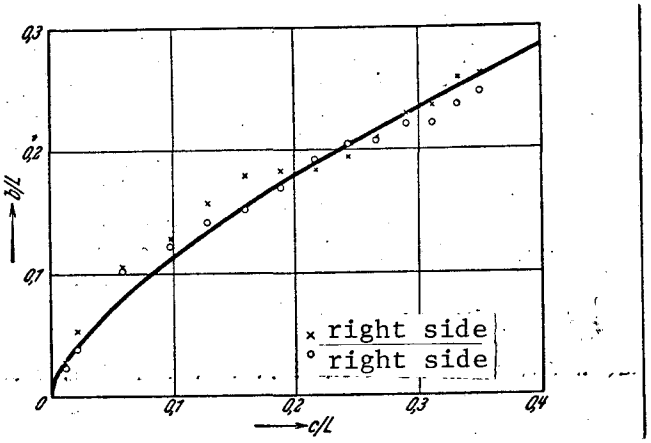

Figure 26. Movement of the vortex in the vertical direction.

This theoretical relation between a/L or b/L and the dimensionless time scale c/L is shown by the solid curves in Figures 25 and 26. The matching values for these quantities / 168
measured from the motion pictures are also plotted, with different designations for the right and left sides. As the theory applies only for the beginning of the movement, the strong deviations of the measured values of a/L from the theoretical curve with increasing c/L (increasing time) are not surprising. For the wing with finite span width (cf. Chapter V) the values must transform into the constant value

$$\frac{a}{L} = \frac{1}{2}\left(1 - \frac{\pi}{4}\right) = 0{,}107$$

asymptotically. This limiting value is shown by the dashed line in Figure 25. The uncertainties of the measured points

are expressed in the differences between the right and left sides, some of which are large. If we consider this uncertainty, we find that the theory is confirmed by the measurements, within the accuracy obtained. Of course, this is for the present limited to the order of magnitude.

Translated for National Aeronautics and Space Administration under contract No. NASw 2035, by SCITRAN, P.O. Box 5456, Santa Barbara, California, 93108